### Title

Spatial Measurement and Inhibition of Calpain Activity in Traumatic Brain Injury with an Activity-Based Nanotheranostic Platform.




### Journal

ACS Nano, 18(37)



### Authors

Madias, Marianne

Stessman, Lilyane

Warlof, Sophia

et al.



### Publication Date

2024-09-17

### DOI

10.1021/acsnano.4c06052

Peer reviewed

ACS NANO

www.acsnano.org



ARTICLE

# Spatial Measurement and Inhibition of Calpain Activity in Traumatic Brain Injury with an Activity-Based Nanotheranostic Platform

Marianne I. Madias, Lilyane N. Stessman, Sophia J. Warlof, Julia A. Kudryashev, and Ester J. Kwon*

Cite This: *ACS Nano* 2024, 18, 25565−25576

Read Online

ACCESS | Metrics & More | Article Recommendations | Supporting Information

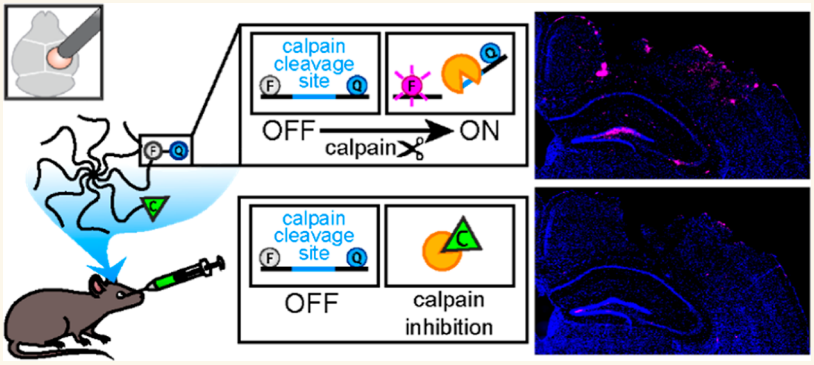


**ABSTRACT:** **Traumatic brain injury (TBI) is a major public health concern that can result in long-term neurological impairments. Calpain is a calcium-dependent cysteine protease that is activated within minutes after TBI, and sustained calpain activation is known to contribute to neurodegeneration and blood−brain barrier dysregulation. Based on its role in disease progression, calpain inhibition has been identified as a promising therapeutic target. Efforts to develop therapeutics for calpain inhibition would benefit from the ability to measure calpain activity with spatial precision within the injured tissue. In this work, we designed an activity-based nanotheranostic (ABNT) that can both sense and inhibit calpain activity in TBI. To sense calpain activity, we incorporated a peptide substrate of calpain flanked by a fluorophore/quencher pair. To inhibit calpain activity, we incorporated calpastatin peptide, an endogenous inhibitor of calpain. Both sensor and inhibitor peptides were scaffolded onto a polymeric nanoscaffold to create our ABNT. We show that in the presence of recombinant calpain, our ABNT construct is able to sense and inhibit calpain activity. In a mouse model of TBI, systemically administered ABNT can access perilesional brain tissue through passive accumulation and inhibit calpain activity in the cortex and hippocampus. In an analysis of cellular calpain activity, we observe the ABNT-mediated inhibition of calpain activity in neurons, endothelial cells, and microglia of the cortex. In a comparison of neuronal calpain activity by brain structure, we observe greater ABNT-mediated inhibition of calpain activity in cortical neurons compared to that in hippocampal neurons. Furthermore, we found that apoptosis was dependent on both calpain inhibition and brain structure. We present a theranostic platform that can be used to understand the regional and cell-specific therapeutic inhibition of calpain activity to help inform drug design for TBI.**

**KEYWORDS:** *calpastatin, activity-based nanosensor, polyethylene glycol, controlled cortical impact, TUNEL*

Over 2.8 million Americans suffer from traumatic brain injury (TBI) every year, and over 5 million people live with a TBI-related disability in the United States.[1,2] However, there are no available therapeutics to treat the long-term brain health in TBI, despite numerous clinical trials.[3] Notably, large multi-center clinical trials for progesterone in TBI failed to establish efficacy as an acute stage neuroprotective treatment.[4,5] A retrospective analysis identified that there is a need for tools to

Received: May 8, 2024
Revised: August 15, 2024
Accepted: August 16, 2024
Published: September 5, 2024

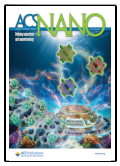

measure target engagement during treatment in order to monitor therapeutic efficacy.[6−8] Moreover, the brain regions that TBI affects can vary due to the location and severity of injury and the underlying susceptibility of each region to injury; therefore, the spatial resolution of injury signals and therapeutic responses may inform the development of therapeutics for TBI.

TBI initiates a secondary injury that unfolds over minutes to days after the primary injury and involves a cascade of events such as protease activation, oxidative stress, immune cell activation, and upregulation of inflammatory cytokines.[9,10] Activated proteases contribute to the degradation of matrix proteins, neurodegeneration, and blood−brain barrier breakdown.[11] Of ectopically activated proteases in TBI, calpains 1 and 2 are calcium-dependent cysteine proteases that are typically intracellular and expressed in neurons, glia, and endothelial cells of the brain. Calpain is activated within minutes after TBI by dysregulated intracellular calcium, and its sustained activity is correlated with worsened outcomes.[12−15] Based on the important role of calpain in disease progression, calpain inhibitors have been developed as promising therapeutics in the form of small molecules and peptides. In neuronal and hippocampal culture models of injury, calpain inhibitors I, II, and III have been used to reduce cell apoptosis, suppress actin and spectrin proteolysis, and inhibit DNA fragmentation.[16−19] In animal models of TBI, these agents can reduce calpain-specific spectrin proteolysis, neuronal cell death, and motor and behavioral deficits; however, their utilization is limited by poor pharmacokinetics and off-target activity.[11,20−27] For example, calpain inhibitor II required continuous intra-arterial infusion after TBI to significantly reduce neurofilament and spectrin proteolysis in the cortex and was not specific to calpains over cathepsins ($K_i$ for calpain-1 = 120 nM, $K_i$ for calpain-2 = 230 nM, $K_i$ for cathepsin B = 100 nM, and $K_i$ for cathepsin L = 600 pM).[13,24] Treatment with multiple doses of the calpain inhibitor III, MDL-28170, both intravenously and intraperitoneally after controlled cortical impact (CCI) in mice was able to reduce spectrin proteolysis by 40% in the ipsilateral hippocampus and 44% in the ipsilateral cortex 24 h post injury ($K_i$ for calpain = 10 nM and $K_i$ for cathepsin B = 25 nM).[20,28] More recently, calpain-2-specific inhibitors have been developed; NA101 ($K_i$ for calpain-1 = 1.3 $\mu$M and $K_i$ for calpain-2 = 25 nM) has been shown to reduce cell death, inflammation, and lesion volume when delivered 1 h after CCI and improve cognitive and motor function after continuous subcutaneous delivery of NA101 over 15 days during repeated mild TBI.[22,29−31] Calpastatin peptide (CAST) is based on the sequence of human calpastatin, an endogenous protein that inhibits calpain ($K_i$ for calpain = 42.6 nM and $K_i$ for cathepsin L = 6 $\mu$M).[32−35]

In studying calpain inhibition and activity, studies typically rely on measuring the bulk concentrations of proteolytic byproducts in brain tissue homogenates. However, the brain is a heterogeneous tissue, and injury pathophysiology with respect to calpain activity and inhibition can vary by brain region.[36−40] For example, calpain activity as measured by spectrin breakdown products (SBDP) has been detected primarily in the cortical and hippocampal regions early after injury, with delayed activation in the thalamus.[41,42] Further, these differences in calpain activity affect regional levels of neurodegeneration and cell death. Neurodegeneration and apoptosis are present acutely after injury in the cortex and hippocampus, appearing later in the thalamus and corpus callosum.[36,43,44] There is evidence that calpain inhibition can also vary by region, although it has not been studied extensively due to a lack of tools. Delivery of a calpain-2 inhibitor in a mouse model of TBI reduced SBDP levels when measured in bulk homogenized cortical tissue, whereas a regional tissue analysis in sectioned brains showed that SBDP was still elevated in the 170 $\mu$m margin from the injury lesion.[22] This elevation of SBDP in the margin corresponded with an elevation in cell death that could not be rescued by a calpain inhibitor. Therefore, understanding calpain inhibition in region- and cell-specific contexts in the brain may inform the design and translation of calpain inhibitors for the therapeutic treatment of TBI.

While calpain mRNA or protein levels can be measured through conventional means, calpain activity is modulated by a variety of factors in its microenvironment, such as cofactors, inhibitors, and spatial localization.[45] Therefore, measurements of calpain activity in bulk assays may not reflect calpain activity in native tissue. The current gold standard for measuring protease activity is gel zymography.[46,47] Quantitative gel zymography can be performed by comparing samples to known standards of the recombinant protease. However, as a bulk technique, spatial information is lost in gel zymography. In a variation of the technique, *in situ* gel zymography can be used to resolve spatial protease activity by overlaying fluorescently labeled protease substrate on tissue sections. However, this method is applied on *ex vivo* samples and therefore may not be able to fully recapitulate the biology of an intact whole organism.[48,49] Activity-based probes have emerged as a small molecule tool for the analysis of protease activity as opposed to protein abundance.[50] These consist of a reactive group that covalently binds to the catalytic residue of the protease active site linked to a tag that enables a downstream assay of tagged proteases. However, the development of sensitive and specific probes can be laborious. To facilitate *in vivo* protease activity measurements for diagnostic use, activity-based nanosensors (ABNs) have been developed.[51−53] In the context of TBI, we have developed an ABN that measures calpain activity after systemic administration.[12,54,55] This technology consists of a peptide substrate for calpain flanked by a fluorophore/quencher pair attached to a 40 kDa 8-arm polyethylene glycol (PEG) scaffold. The nanoscale PEG scaffold allows for passive accumulation in the injured brain due to its extended blood circulation time and nanometer size.[12,55] We have shown that this nanosensor is able to measure calpain activity with spatial precision in brain slices and whole brains,[12,54] is compatible with cell type-specific staining,[12,54] and its activation correlates with TBI severity.[55]

In this work, our goal was to create an activity-based nanotheranostic for TBI (TBI−ABNT) that can both sense and inhibit calpain activity. We attached CAST, a peptide inhibitor to calpain, and calpain sensor (CS) peptide to a PEG scaffold. CAST is taken from a domain of calpastatin, an endogenous inhibitor of calpain, and has been investigated as a therapeutic to reduce calpain-mediated proteolysis and behavioral deficits after TBI.[11,20,21,56−58] Physically tethering CAST and CS peptides to the same scaffold allows us to elucidate interactions between calpain and CAST in the microenvironment that would not be possible with the codelivery of each individual peptide due to their disparate biodistribution. We establish that the addition of CAST onto the construct can inhibit activation of the CS peptide in the


https://doi.org/10.1021/acsnano.4c06052
ACS Nano 2024, 18, 25565−25576

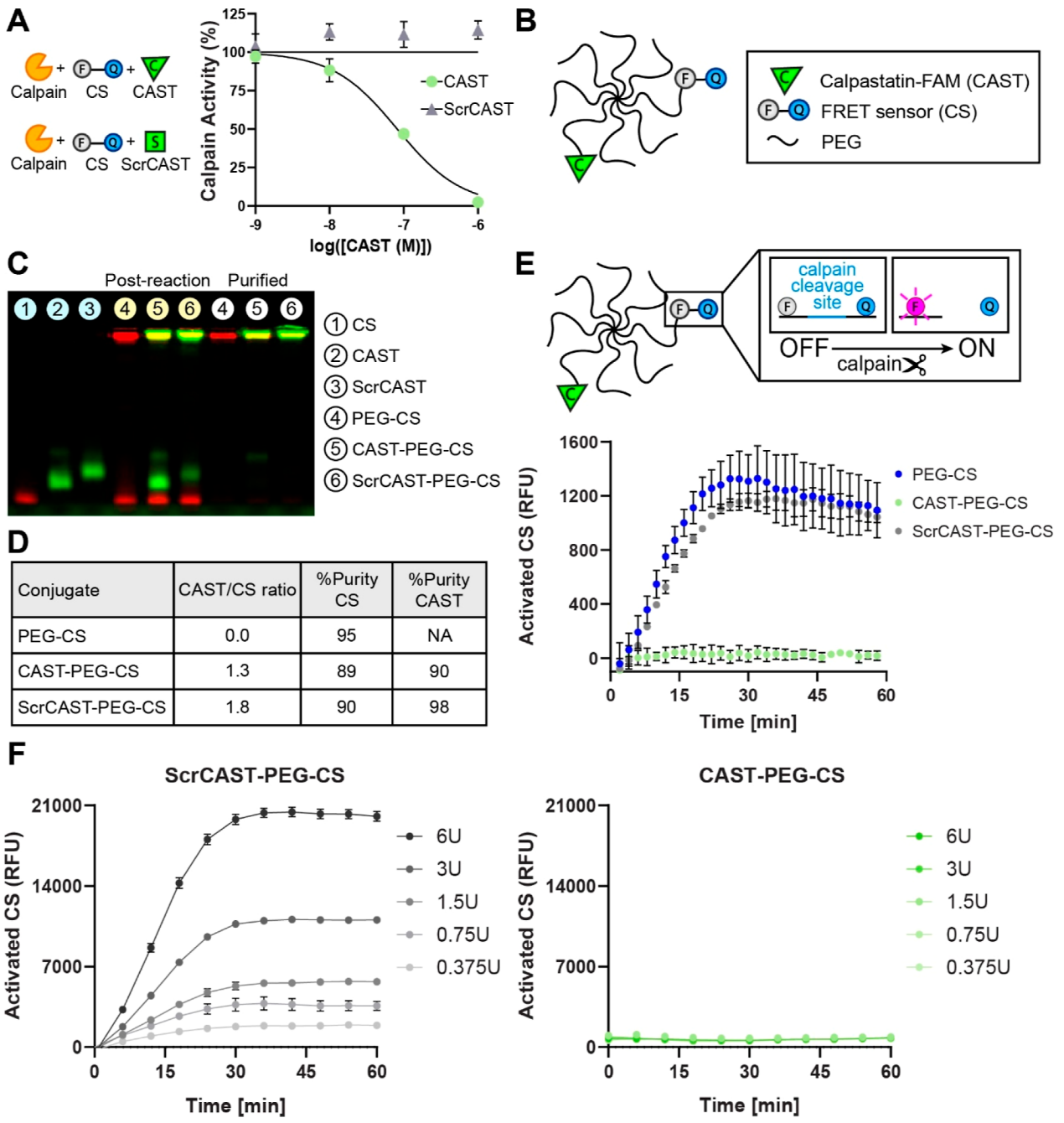


| Conjugate | CAST/CS ratio | %Purity CS | %Purity CAST |
|---|---|---|---|
| PEG-CS | 0.0 | 95 | NA |
| CAST-PEG-CS | 1.3 | 89 | 90 |
| ScrCAST-PEG-CS | 1.8 | 90 | 98 |

**Figure 1. Synthesis and characterization of calpain nanotheranostic. (A) Titration of CAST for calpain-1 inhibition. (B) Schematic of nanotheranostic composed of a PEG nanomaterial scaffold, CAST, and CS peptide. (C) Gel comparing free CS peptide, CAST, and ScrCAST peptide to PEG−CS, CAST−PEG−CS, and ScrCAST−PEG−CS conjugates before and after purification by dialysis. (D) Relative amounts of CAST/ScrCAST peptide to CS peptide on nanotheranostic conjugates and purity of conjugates by CS and CAST/ScrCAST. (E) Schematic of substrate peptide activation by calpain. CS activation of nanotheranostic materials was performed by recombinant human calpain-1. (F) Measurements of CS activation at various concentrations of calpain-1 over 1 h.**

presence of recombinant calpain, whereas the addition of a CAST scrambled peptide does not. When dosed intravenously in a mouse model of TBI, we found that our TBI−ABNT material has access to ectopic calpain activity in the injured perilesional tissue. Analysis of CS peptide activation in brain slices showed that our nanotheranostic reduced calpain activation in neurons, endothelial cells, and microglia of the cortex and, to a lesser degree, neurons in the hippocampus. When we measured apoptosis, we saw reduced cell death in the cortex, consistent with the regional activation measurements from our nanotheranostic. While we did see inhibition of calpain activity in the hippocampus, we did not see reductions in apoptosis. Therefore, our ABNT tool elucidates regional differences of how calpain activity and its inhibition impact apoptosis acutely after injury. In summary, we have engineered a theranostic technology that can be used for regional- and cell-specific measurement and inhibition of calpain activity in TBI. Furthermore, a calpain activity biomarker tool has the potential to be used to understand the regional- and cell-specific


https://doi.org/10.1021/acsnano.4c06052
ACS Nano 2024, 18, 25565−25576

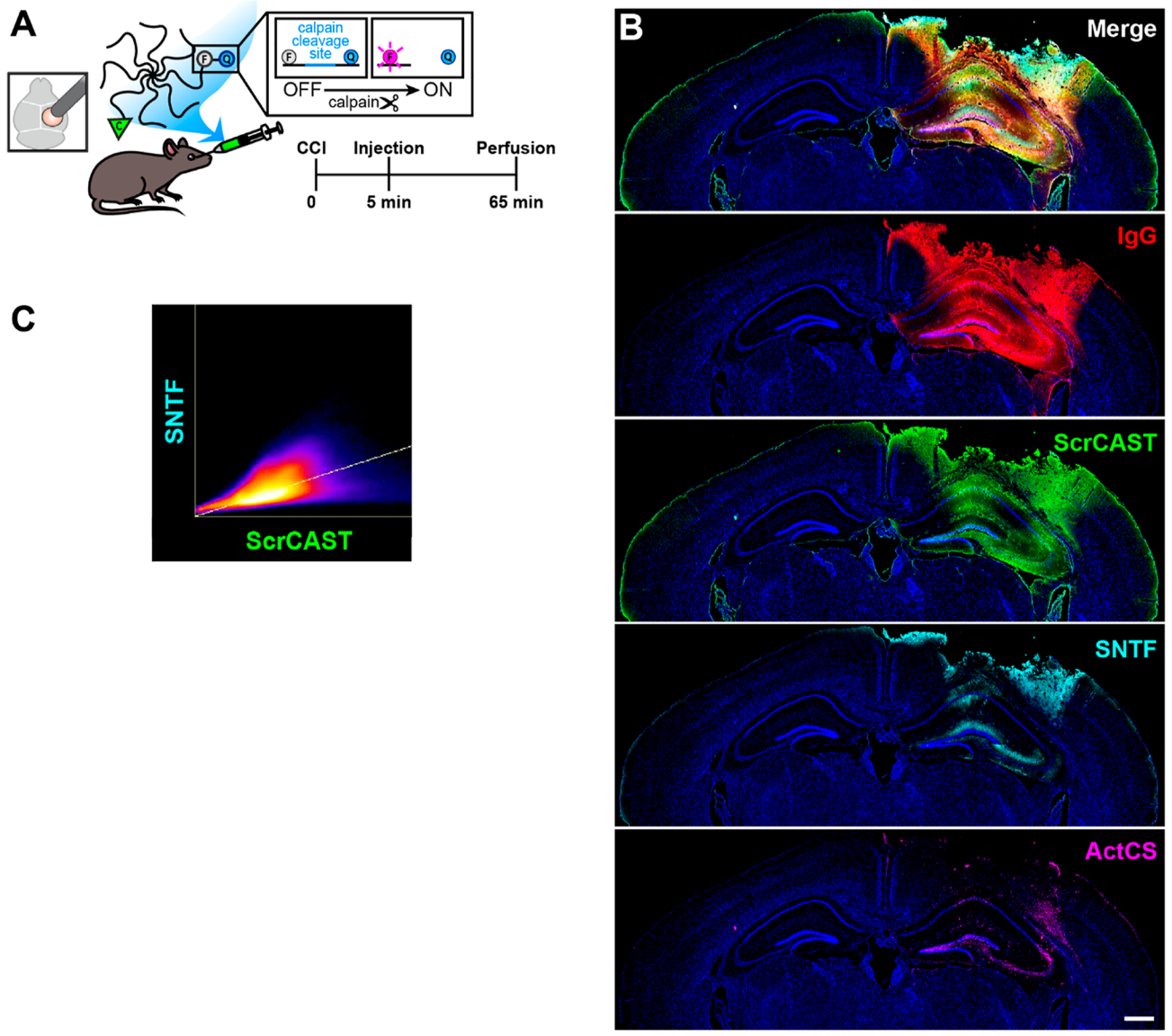


**Figure 2. ScrCAST−PEG−CS has widespread distribution in the injured brain where there is dysregulated vasculature and calpain activity. (A) Overview of the experimental timeline. (B) Coronal brain sections of mice administered ScrCAST−PEG−CS and stained for endogenous IgG, FAM, and cleaved spectrin (red, IgG; green, FAM-labeled nanomaterial; cyan, SNTF; magenta, activated CS peptide; scale bar = 500 $\mu$m). (C) Scatterplot showing colocalization of pixels positive for FAM on the ScrCAST peptide and cleaved spectrin (SNTF).**

therapeutic efficacy of drugs and to help inform the clinical development of drugs for TBI.

## RESULTS AND DISCUSSION

**Calpain Nanotheranostic Is Able to Sense and Inhibit Calpain Activity.** Our goal was to create a theranostic nanomaterial that could both inhibit and measure calpain activity. We first validated the activity of a peptide inhibitor of calpain using the inhibitory domain of the endogenous calpain inhibitor, calpastatin.[59,60] This calpastatin peptide (CAST; sequence: DPMSSTYIEELGKREVTIPPKYRELLA) was synthesized with a fluorescein (FAM) label for quantification and an N-terminal cysteine for conjugation to the 8-arm PEG scaffold via maleimide chemistry. In order to create a control material that does not inhibit calpain, we synthesized in parallel a material modified with a scrambled CAST peptide (ScrCAST). We titrated CAST and ScrCAST peptide concentrations and measured the cleavage of a calpain-specific FRET sensor peptide (CS) in the presence of recombinant human calpain-1 enzyme (Figure 1A). The CS peptide substrate sequence was taken from $\alpha$-spectrin, an endogenous substrate of both calpain-1 and -2[61,62] that we have previously validated for calpain-specific cleavage.[12] We demonstrate that the CAST peptide is able to inhibit calpain-1 activity with a 50% inhibitory concentration ($IC_{50}$) of ∼100 nM, and ScrCAST does not have any detectable inhibitory activity up to 1 $\mu$M (Figure 1A). This is comparable to other calpain inhibitors such as calpain inhibitor I ($IC_{50}$ = 90 $\mu$M),[63] MDL-28170 ($IC_{50}$ = 11 nM),[64] and NA101 ($IC_{50}$ = 1130 nM).[31]

After validating the inhibitory activity of CAST peptide, we synthesized a calpain activity inhibitor/sensor nanotheranostic by modifying a 40 kDa 8-arm PEG scaffold with CAST and CS peptide (Figure 1B). In previous work, we have demonstrated that systemically administered 40 kDa 8-arm PEG has access to the injured brain.[12] PEG−CS, CAST−PEG−CS, and ScrCAST−PEG−CS conjugates were synthesized by batch


https://doi.org/10.1021/acsnano.4c06052
ACS Nano 2024, 18, 25565−25576

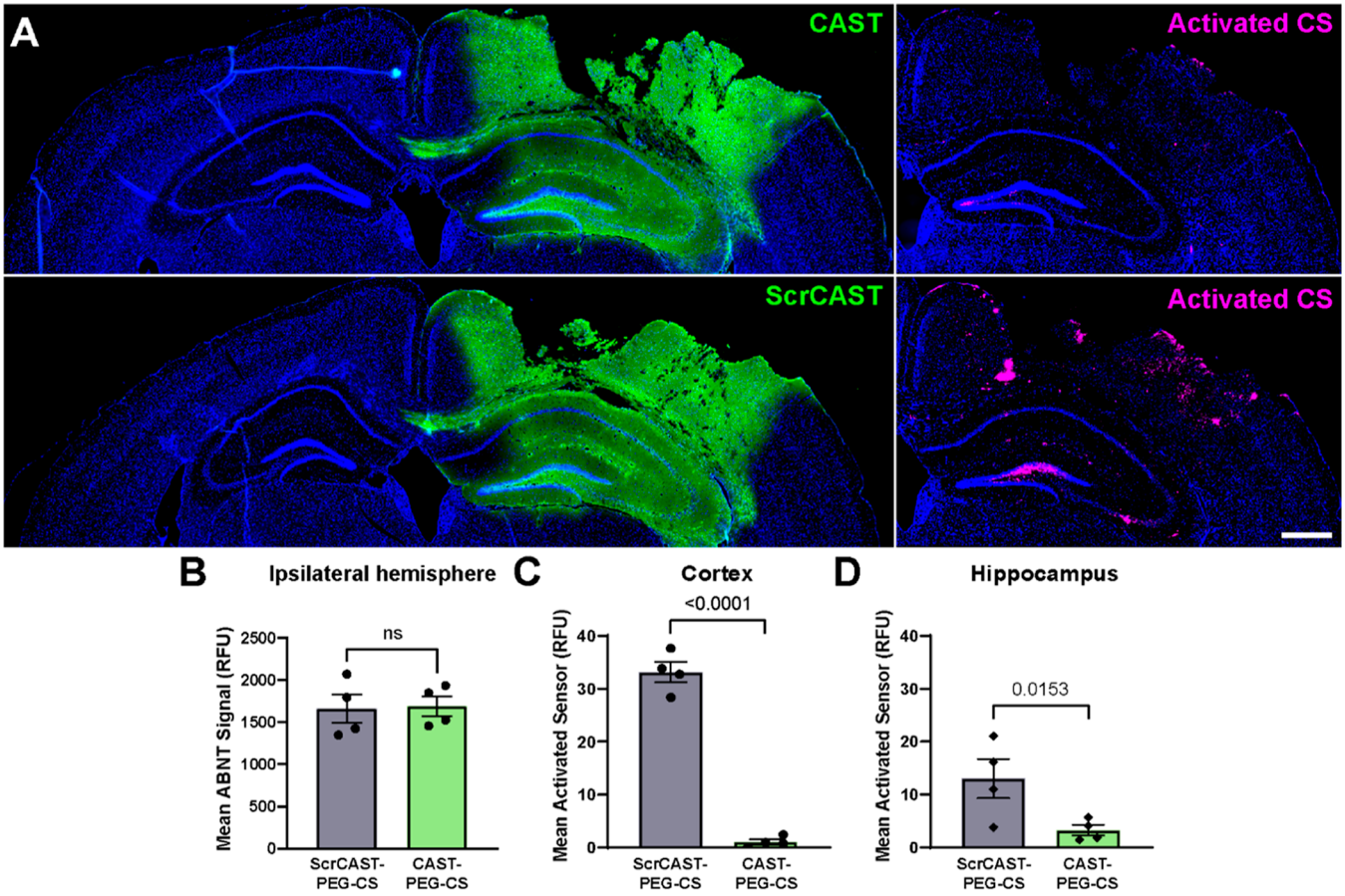


**Figure 3. CAST−PEG−CS has widespread distribution in the injured brain and inhibits CS sensor signal in a mouse model of TBI. (A) Coronal brain sections collected from mice 1 h after CAST−PEG−CS or ScrCAST−PEG−CS administration and imaged for FAM on the CAST/ScrCAST peptide (green) and activated CS peptide (magenta; scale bar = 500 $\mu$m). (B) Quantification of mean FAM signal on the ScrCAST/CAST peptide in the brain ipsilateral to injury after ScrCAST−PEG−CS or CAST−PEG−CS delivery ($n$ = 4, mean ± SEM, unpaired $t$-test). Quantification of mean activated CS signal in the injured (C) cortex or (D) hippocampus after ScrCAST−PEG−CS or CAST−PEG−CS delivery ($n$ = 4, mean ± SEM, unpaired $t$-test).**

reacting 40 kDa 8-arm PEG with CS peptide, splitting the reaction into three portions, and adding L-cysteine, CAST, or ScrCAST peptide. Therefore, the amount of CS peptide per PEG was the same for each material. The resulting conjugates were purified by dialysis to remove the unconjugated peptide. After dialysis, conjugates had little to no detected unreacted CS or CAST/ScrCAST peptide (Figure 1C,D). We quantified the relative amount of CAST/ScrCAST to the CS peptide by the absorbance of FAM and Cy5 fluorophores, respectively. We measured ∼1.5 CAST/ScrCAST peptide to CS peptide, indicating a similar level of CAST/ScrCAST substitution since PEG was batch reached with CS peptide prior to CAST/ScrCAST reaction (Figure 1D).

To measure the activity of the synthesized conjugates *in vitro*, PEG−CS, CAST−PEG−CS, and ScrCAST−PEG−CS were incubated with recombinant human calpain-1. Calpain cleavage activity was detected by measuring the dequenched Cy5 fluorescence signal over time (Figure 1E). As expected, both PEG−CS and ScrCAST−PEG−CS are cleaved by active calpain, resulting in increasing Cy5 fluorescence over time. ScrCAST−PEG−CS has a similar activation profile to PEG-CS, demonstrating that ScrCAST peptide does not inhibit calpain activity. There was no measured activation of CS peptide from the CAST−PEG−CS conjugate, demonstrating the inhibition of calpain activity with the CAST peptide. Calpain-1 concentrations up to 6U (equivalent to ∼380 nM, >10-fold higher than physiologic calpain concentrations[65]) were used to test CAST−PEG−CS inhibition (Figure 1F). Even at high levels of calpain-1, CAST−PEG−CS was able to inhibit activity and cleavage of the CS substrate compared to ScrCAST−PEG−CS. These results establish that CAST−PEG−CS can inhibit calpain, and ScrCAST−PEG−CS is an effective control material with no inhibitory activity. Together, these constructs can be used to measure calpain activity and inhibition.

**Calpain Nanotheranostic Accumulates within Injured Brain Tissue in Areas with Calpain Activity.** We first validated that our conjugate can access relevant perilesional brain tissue *in vivo* after a CCI, a mouse model of TBI. CCI is a well-controlled and reproducible model of TBI injury, and calpain activity elevates within minutes after CCI.[13,66] We performed CCI injuries with preoperative analgesia by exposing dura through a 5 mm diameter craniotomy and impacting with a 2 mm diameter probe at a speed of 3 m/s and a depth of 2 mm. We delivered 5 nmoles of ScrCAST−PEG−CS and CAST−PEG−CS matched by CS concentration via retro-orbital injection 5 min post-CCI to capture acute calpain activity since it is known that calpain is detected as early as 30 min after injury.[12,13] 1 h after conjugate administration, mice were perfused with fixative and brains were collected (Figure


https://doi.org/10.1021/acsnano.4c06052
ACS Nano 2024, 18, 25565−25576

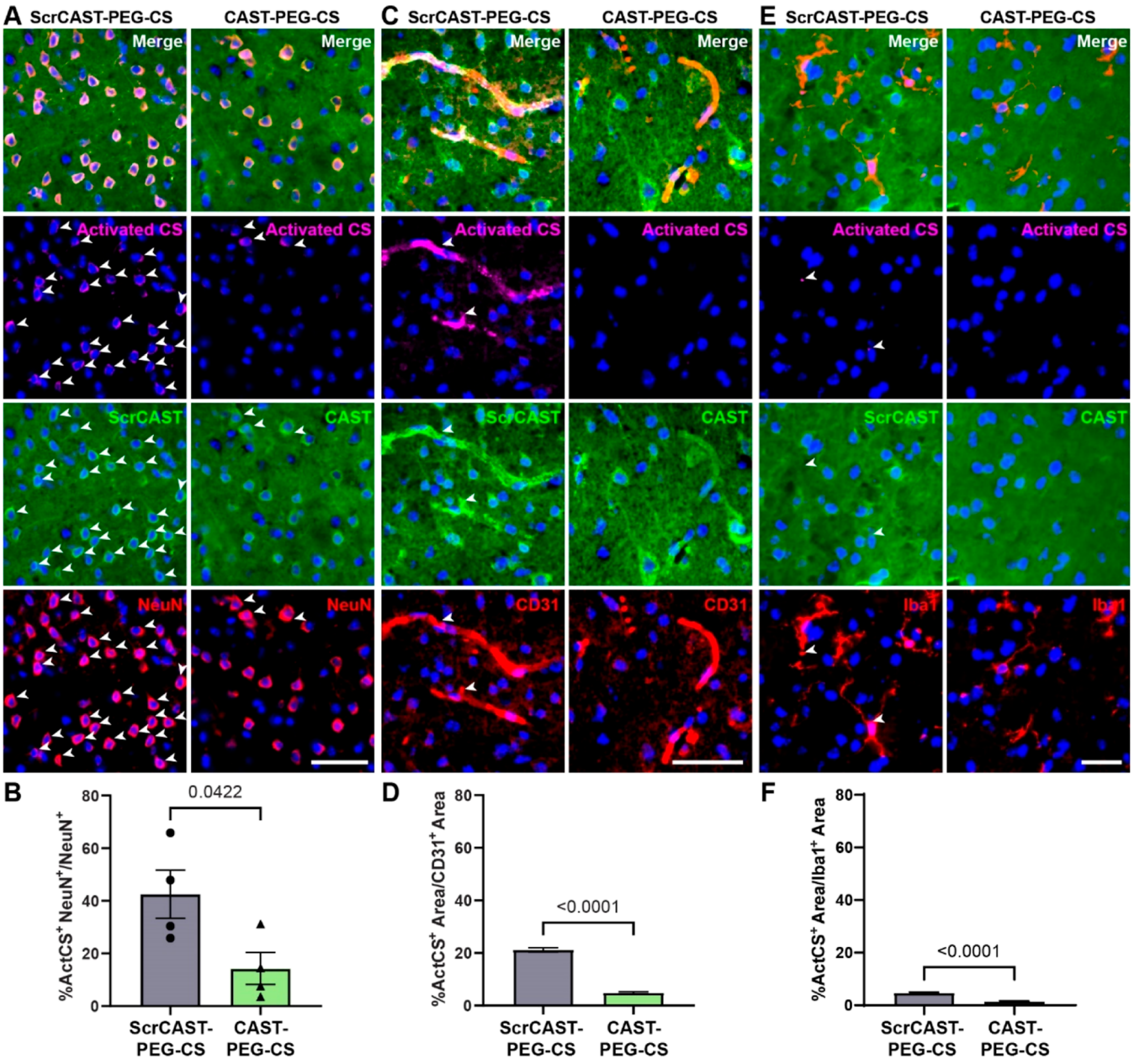


**Figure 4. CAST delivery inhibits the activation of CS in neurons, vasculature, and microglia in the injured cortex. ScrCAST−PEG−CS and CAST−PEG−CS conjugates (green) and activated CS peptide (magenta) in the injured cortex assessed 1 h after delivery stained for (A) neurons (red, NeuN), (B) endothelial cells (red, CD31), and (C) microglia (red, Iba1) (scale bars = 50 $\mu$m). Arrows denote activated sensor (magenta) in each cell type. Quantification of percent (B) neurons, (D) endothelial cells, and (F) microglia positive for activated CS peptide in the injured cortex ($n$ = 4 mice, mean ± SEM, unpaired $t$-test).**

2A). Coronal sections from the center of the injury were stained with an anti-FAM antibody for the CAST/ScrCAST peptides to evaluate the spatial distribution of conjugates in the brain (Figure 2B). Sections were stained for anti-IgG antibody to visualize IgG extravasation in injured tissue; IgG extravasation has been used to identify BBB damage in the perilesional tissue.[67,68] The regional distribution of FAM-labeled nanomaterials corresponded well with extravasated IgG. Sections were also stained with an antibody specific for the N-terminal proteolytic fragment of spectrin (SNTF), known to be generated by calpain-specific cleavage and, therefore, a marker of calpain activity. A scatter plot of colocalized pixels indicates that all pixels positive for SNTF are also positive for our nanomaterial (Figure 2C), which supports that our construct can adequately sample ectopic calpain activity in the injured brain. These results demonstrate that our nanomaterial can access relevant injured perilesional tissue after systemic administration.

**Calpain Nanotheranostic Inhibits Calpain Activity in a Mouse Model of TBI.** We next asked whether our nanotheranostic was capable of inhibiting and measuring calpain activity *in vivo* after CCI. We first verified that our ABNT can passively accumulate in the injured hemisphere of the brain to a similar extent as our control material after 1 h of circulation (Figure 3A). We observed that both CAST−PEG−CS and ScrCAST−PEG−CS conjugates have similar distributions in the injured cortex and hippocampus, and therefore differences in the activated CS signal are not due to differences


https://doi.org/10.1021/acsnano.4c06052
ACS Nano 2024, 18, 25565−25576

in conjugate distribution but to differences in calpain activity. Quantification of the FAM signal in the brain ipsilateral to injury shows nonsignificant differences in accumulated material between ScrCAST−PEG−CS and CAST−PEG−CS (Figure 3B). The activated CS sensor was visualized by the fluorescence signal from the dequenched Cy5 fluorophore in tissue sections. ScrCAST−PEG−CS showed distinct activation of the CS peptide in the injured cortex and hippocampus, consistent with our previous work.[12,54] By contrast, CAST−PEG−CS showed markedly less CS peptide activation in the injured brain compared with ScrCAST−PEG−CS, indicating an inhibition of calpain activity. Furthermore, quantification of CS peptide activation signal by region shows a ∼33-fold increase in the cortex and only a ∼4-fold increase in the hippocampus when comparing between constructs with ScrCAST vs CAST (Figure 3C,D), indicating a differential inhibition of calpain activity across these two brain regions. Our results are consistent with reports of differential inhibition of calpain activity in the cortex and hippocampus post-CCI in a transgenic mouse model overexpressing calpastatin.[21]

**Calpain Nanotheranostic Inhibits Calpain Activity within Cortical Cells.** To further investigate ABNT-mediated cell-specific calpain inhibition in the cortex, we measured CS activation in neurons, endothelial cells, and microglia 1 h after injury. Neurons and endothelial cells are a major source of calpain and activated neuronal and endothelial calpain can lead to neurodegeneration and blood−brain barrier breakdown after injury.[11,12,17,54,69−71] We analyzed neurons, endothelial cells, and microglia in the perilesional cortex, a region with major tissue loss acutely after injury and therefore an important region for therapeutic delivery.[20,72] CAST/ScrCAST colocalized with NeuN and CD31 positive cells, supporting that the conjugate is localized to neurons and endothelial cells and therefore can be used to detect intracellular calpain activity (Figure 4A−D). Quantification revealed that the number of cortical neurons with activated CS decreased more than 50% after CAST−PEG−CS treatment compared with ScrCAST−PEG−CS treatment (Figure 4B). Quantification of the percent area of endothelial cells colocalized with activated CS shows that CAST−PEG−CS treatment reduces the area of activated CS in the vasculature by over 4-fold (Figure 4D). This suggests that the CAST peptide significantly inhibits calpain activity in cortical neurons and endothelial cells after injury. These results correlate with previous work that showed delivery of a calpain inhibitor in rats post-CCI led to reduced neurofilament staining in cortical neurons.[24] In a mouse model, treatment with a calpain inhibitor led to reduced Evans blue dye leakage 1 h post-CCI, demonstrating a protective effect of calpain inhibition on endothelial hyperpermeability following injury.[11] Although there is colocalization of ABNT with Iba1-labeled microglia, there is little ABNT activation (Figure 4E,F). This is unsurprising as there is very little literature on calpain activity in microglia after TBI.[65,73] Our data support the use of our nanotheranostic to monitor inhibition of calpain activity in neurons and endothelial cells, two major cell types implicated in the secondary injury of TBI. An advantage of our ABNT technology over the measurement of endogenous SBDP is that the time period of calpain activity measurements can be controlled through the administration and measurement times, whereas the measurement of SBDP is cumulative from the initiation of injury.

**Calpain Nanotheranostic Inhibits Calpain Activity in the Hippocampus.** We next analyzed our nanotheranostic in the hippocampus. The hippocampus is the major structure for learning and memory and hippocampal neurons are particularly susceptible after TBI.[16,21,41,42,69,72,74−76] Therefore, the hippocampus is an important structure to target for therapeutic delivery. While cell counting is challenging to accomplish in the hippocampus due to the high density of neuronal bodies, different regions of the hippocampus are responsible for functional deficits after TBI, and therefore we performed regional analysis in the dentate gyrus, CA1, CA2, and CA3. FAM-labeled CAST/ScrCAST nanomaterial was found throughout the hippocampus 1 h after injury (Figure 5A). Activated CS peptide was observed throughout all regions of the hippocampus after ScrCAST−PEG−CS delivery, indicating calpain activity in the perilesional hippocampus. By contrast, after the delivery of CAST−PEG−CS, there is significantly less activation of the sensor in the CA1, CA2, and CA3 regions of the hippocampus at 1 h after injury (Figure 5B). Notably, sensor activation was high in the dentate gyrus compared to the other regions in the hippocampus, and ABNT delivery had less of an impact on reducing calpain activity than in the other hippocampal regions. Our results correlate with previous work showing a high number of degenerating neurons and breakdown products in neurons of the dentate gyrus compared to CA3 and CA1 after CCI.[21,37,75,76] Fluoro-jade B staining for degenerating neurons in the hippocampus after injury shows that degenerating neurons are primarily localized in the dentate gyrus and are not rescued by calpastatin overexpression in a severe CCI model.[21] Our study supports that there is robust calpain activity in the dentate gyrus after TBI, and therefore higher therapeutic concentrations of the calpain inhibitor may be needed for effective inhibition of calpain in this region.

**Calpain Nanotheranostic Reduces the Number of Apoptotic Cells in Injured Cortex.** After determining that CAST delivery reduces calpain activity post-CCI in the injured cortex and hippocampus with our nanotheranostic technology, we next investigated whether calpain inhibition could prevent cell death. After TBI, there is an increase in the number of apoptotic cells stained by TUNEL at acute time points in the cortex and after 24 h in the hippocampus and thalamus.[22,43,44,77] Studies *in vitro* have shown that calpain inhibitors rescue neuronal cultures from apoptosis and delivery of a calpain-2 inhibitor in mice after TBI reduced the number of both TUNEL-positive and Fluoro-Jade C-positive neurons around the lesion after injury.[16,17,19,22] Therefore, we hypothesized that a reduction of calpain activity in neurons in the cortex could partially prevent these cells from apoptosis at acute time points after TBI. Apoptosis was measured by TUNEL on brain sections 1 h after delivery of CAST−PEG−CS or ScrCAST−PEG−CS (Figure 6A). Quantification of the amount of TUNEL positive area showed that CAST significantly reduced the number of apoptotic cells in the injured cortex by ∼50% (Figure 6B). By contrast, no differences were observed in the TUNEL positive area in the hippocampus (Figure 6C). The overall amount of TUNEL positive area in the hippocampus was relatively low, consistent with studies showing that calpain breakdown products and apoptotic cells in the hippocampus do not increase until 24 h after injury.[36,42,44] Interestingly, our ABNT technology demonstrated that while calpain activity and TUNEL were correlated and could be modulated by calpain inhibition in the cortex, these measurements were decoupled in the hippocampus. The dentate gyrus in the hippocampus is a center of


https://doi.org/10.1021/acsnano.4c06052
ACS Nano 2024, 18, 25565−25576

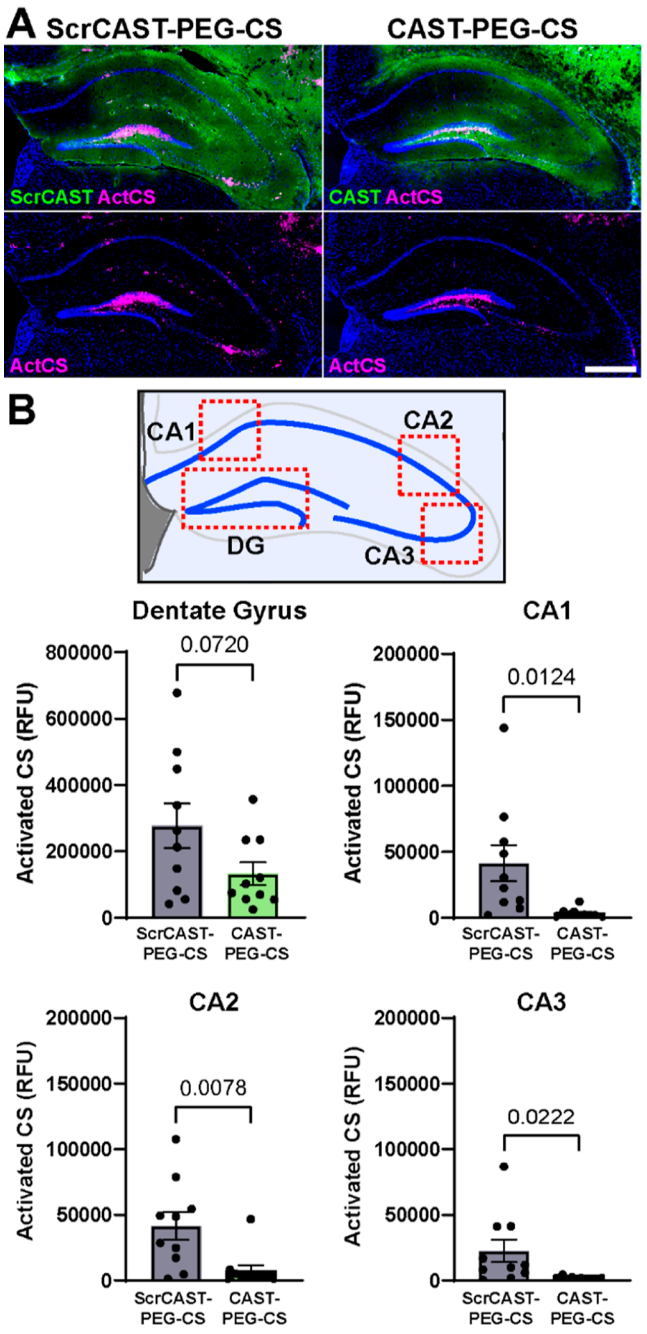


**Figure 5. CAST inhibits activation of CS in the injured hippocampus. (A) Microscopy images of ScrCAST−PEG−CS and CAST−PEG−CS conjugates (FAM, green) and activated sensor (Cy5, magenta) in the hippocampus ipsilateral to injury 1 h after injury (scale bar = 500 $\mu$m.) (B) Quantification of activated CS peptide in the dentate gyrus, CA1, CA2, and CA3 regions denoted by the dotted red boxes in the schematic ($n$ = 10 mice, mean ± SEM, unpaired $t$-test).**

neurogenesis, and newborn neurons have been shown to be more resistant to cell death than mature neurons,[78−80] which may explain in part why CAST does not reduce TUNEL staining in the hippocampus even though it does decrease calpain activity at acute time points (Figure 5). In summary, our ABNT technology enabled observations of region-specific differences in calpain activation, calpain inhibition, and calpain-mediated neurodegeneration in TBI. Such tools that can spatially probe calpain activity and inhibition may be useful in elucidating the role of calpain in secondary injury after TBI.

## CONCLUSIONS

We engineered a calpain nanotheranostic that could both measure and inhibit calpain activity with spatial specificity at the cellular and regional levels in the brain. Furthermore, we observed that calpain inhibition can reduce the number of apoptotic cells in a region-specific manner; in the cortex, inhibition of calpain activity correlated with a decrease in apoptosis, whereas in the hippocampus, cells appeared to be more resistant to apoptosis, independent of calpain activity. We believe our technology could be used as a tool to further develop calpain inhibitors as a class of therapeutics for TBI. Due to the central role of calpain activity in multiple disease pathways active during secondary injury, spatial measurements of calpain activity could also be used as a biomarker for therapeutics beyond calpain inhibitors. While calpain activity as a single measurement does not capture the full picture of disease in the brain after TBI, we believe our technology is an example of how precise spatial coupling of therapeutic molecules and their target engagement can contribute to the understanding of their function. In future work, we could couple measurements from our ABNT with spatial transcriptomics to further understand the contribution of calpain activity and inhibition to gene expression.

## METHODS

**Synthesis of PEG Conjugates.** The calpain-specific substrate FRET CS peptide (QSY21-QEVYGAMP-K(Cy5)-PEG2-GC-NH2) was synthesized by CPC Scientific Inc. (Sunnyvale, CA). PEG2 stands for PEG. The calpastatin (DPMSSTYIEELGKREVTIPPKYRELLA-K(5FAM)-C-NH2) and scrambled calpastatin (APRLEIVPT-MYIYKLSPTGSEKLEDER-K(5FAM)-C-NH2) peptides were synthesized by LifeTein (Somerset, NJ). The 40 kDa 8-arm PEG maleimide (tripentaerythritol core) was purchased from JenKem Technology (Beijing, China). The 8-arm PEG maleimide was reacted with 1 mol equivalent of calpain substrate FRET peptide in the presence of 50 mM triethylamine, split into 3 batches, and reacted with 0 mol equivalent of CAST, 3 mol equivalent of CAST, or 3 mol equivalent of scramble CAST. Batches were reacted for 3 h and quenched with an excess of L-cysteine. All conjugates were dialyzed in PBS, and final concentrations were determined by the absorbance of FAM or Cy5 using a Genesys 150 spectrophotometer (Thermo Scientific).

SDS−PAGE was performed with a 12% polyacrylamide gel loaded with CS peptide, CAST peptide, ScrCAST peptide, postreaction PEG−CS, postreaction CAST−PEG−CS, postreaction ScrCAST−PEG−CS, purified PEG−CS, purified CAST−PEG−CS, and purified ScrCAST−PEG−CS. Electrophoresis was performed at room temperature for approximately 45 min using a constant voltage (120 V) in Tris-glycine SDS running buffer. Cy5 fluorescence from the CS peptide was imaged on an Odyssey Scanner (Li-Cor Biosciences), and FAM fluorescence from the CAST/ScrCAST peptide was imaged on a Biorad scanner.

**In Vitro Reaction Kinetics Assay.** Titrated CAST and conjugates matched to 8 $\mu$M CS substrate were incubated with 26.6 nM recombinant human calpain-1 (Sigma-Aldrich, C6108) in 50 mM *N*-(2-hydroxyethyl)piperazine-*N*-ethanesulfonic acid, 50 mM NaCl, 2 mM ethylenediaminetetraacetic acid, 5 mM $CaCl_2$, and 5 mM $\beta$-mercaptoethanol. For the study with increased calpain-1 concentration, 6U of calpain-1 (~380 nM) was used. For the study comparing CAST−PEG−CS inhibition to MDL-28170 (Sigma M6690), 12 $\mu$M of MDL-28170 was used. Fluorescence readings were taken every 120 s at 37C for 1 h or 30 h for long-term study using a Spark multimode microplate reader (Tecan Trading AG,


https://doi.org/10.1021/acsnano.4c06052
ACS Nano 2024, 18, 25565−25576

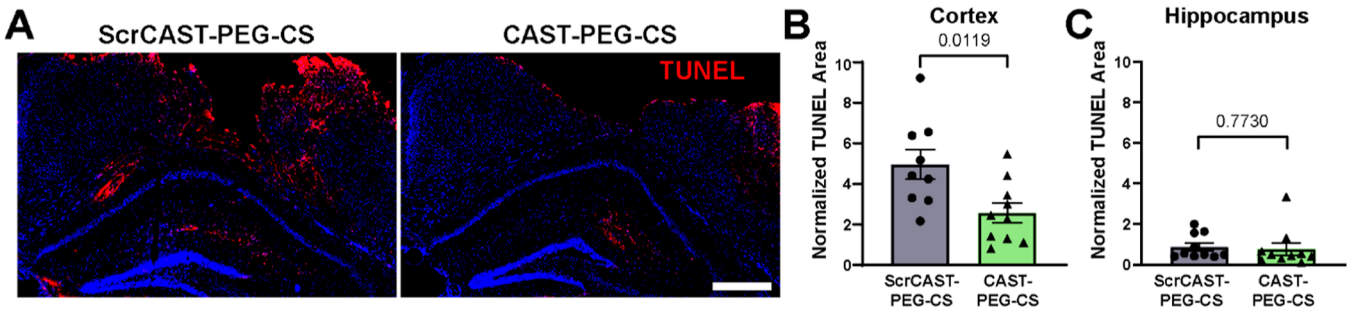


**Figure 6. CAST delivery after injury reduces the number of apoptotic cells in the injured cortex and hippocampus. (A) TUNEL assay performed on coronal brain sections from mice administered ScrCAST−PEG−CS or CAST−PEG−CS (red, TUNEL; blue, nuclei; scale bar = 500 $\mu$m). Quantification of the TUNEL positive area normalized by nuclei area in the injured (B) cortex and (C) hippocampus after ScrCAST−PEG−CS or CAST−PEG−CS administration ($n$ = 10 mice, mean ± SEM, unpaired $t$-test).**

Switzerland). Reaction curves were normalized to controls, and $V_{max}$ values were calculated between 10 and 20 min to fit to a dose−response inhibition curve in GraphPad Prism (10.1.2).

**CCI TBI Mouse Model.** All mouse protocols were approved by the University of California San Diego's Institutional Animal Care and Use Committee. Female C57BL/6J mice (8−12 weeks old, Jackson Laboratories) weighing between 18 and 22 g were used for all in vivo studies. Following anesthetization with 2.5% isoflurane, buprenorphine analgesia was administered. A 5 mm craniotomy was performed over the right hemisphere between the bregma and lambda, and a CCI was performed using the ImpactOne (Leica Biosystems) with a 2 mm diameter stainless steel probe at a velocity of 3 m/s, a depth of 2 mm, and a dwell time of 300 ms. The probe was centered around −2.0 mm (±0.5 mm) lateral from the midline and −2.0 mm (±0.5 mm) caudal from bregma.

**In Vivo Studies.** Five min after CCI, 5 nmol (concentration based on calpain substrate FRET peptide) of ScrCAST−PEG−CS and CAST−PEG−CS in PBS was injected retro-orbitally. Nanomaterial doses were administered to mice in a weight range of 18−22 g, corresponding to a dosage range of 227−278 nmol/kg. Following a 1 h circulation time, mice were sacrificed by transcardial perfusion of USP saline, followed by 10% formalin.

**Immunostaining of Brain Tissue Slices.** Following transcardial perfusion with 10% formalin, necropsied brains were further fixed in 10% formalin at 4C overnight. Brains were washed in PBS, transferred to 30% w/v sucrose in PBS to equilibrate overnight, then frozen in OCT (Tissue-Tek). Coronal tissue slices 10 $\mu$m thick were obtained in the 2 mm diameter injury region and then stained using conventional protocols. Briefly, tissues were blocked for 1 h in 3% bovine serum albumin, 5% serum of secondary antibody, and 0.1% Triton X-100. For NeuN staining, blocking buffer is included 2 $\mu$g/mL of donkey antimouse Fab. The following primary antibodies were used: 1:1000 SNTF (Millipore ABN2264), 1:800 NeuN (Millipore MAB377), 1:200 CD31 (BD 553370), 1:500 Iba1 (Wako 019-19741), and 1:200 FAM (Invitrogen, A889). Primary antibody incubations were done in blocking buffer overnight at 4C. For IgG staining, donkey anti mouse IgG 594 was added during secondary staining. Secondary antibodies were applied for 1 h at room temperature, and the samples were washed in PBS and mounted with a Fluoromount-G instrument (Southern Biotech). Images were collected on a Nikon Eclipse Ti2 microscope fitted with a Hamamatsu Orca-Flash 4.0 digital camera. Sensor distribution was visualized in the FITC channel, and the activated sensor was visualized in the Cy5 channel. Images for direct comparison were collected by using the same exposure and LED intensity settings.

**TUNEL Staining of Brain Tissue Slices.** Tissues were stained with an in situ Cell Death Detection Kit, TMR red (Roche, 12156792910) using conventional protocols. Briefly, tissues were permeabilized in 0.1% Triton X-100 for 30 min and washed in PBS. 1:10 TUNEL enzyme and 1:1000 Hoescht in labeling solution were incubated with tissues at 37C for 1 h. Samples were washed in PBS and mounted with Fluoromount-G (Southern Biotech). Images were collected on a Nikon Eclipse Ti2 microscope fitted with a Hamamatsu Orca-Flash 4.0 digital camera. TUNEL positive staining was visualized in the TXR channel. Images for direct comparison were collected using the same exposure and LED intensity settings.

**Software and Statistics.** GraphPad Prism (10.1.2) was used to perform statistics and QuPath (0.5.0) was used to perform analysis of the percent area of activated CS in endothelial cells and microglia. ImageJ was used to analyze the number of neurons with activated CS. All $t$ tests were conducted with an alpha of 0.05 to identify statistical significance between samples. In the results for the normalized TUNEL area in the cortex, an outlier was removed from the ScrCAST−PEG−CS group using the ROUT method with a maximum false discovery rate of 0.1%. The colocalization threshold plugin on ImageJ was used to generate the scatter plot of the pixel intensity.

## ASSOCIATED CONTENT

### Supporting Information

The Supporting Information is available free of charge at https://pubs.acs.org/doi/10.1021/acsnano.4c06052.

Cleavage of PEG−CS, ScrCAST−PEG−CS, and CAST−PEG−CS by recombinant calpain-1 over 30 h; inhibition of ScrCAST−PEG−CS cleavage by MDL-28170; specificity of CS cleavage for recombinant calpain-1 over caspase-3; percent positive SNTF staining in the ipsilateral and contralateral cortex and hippocampus; and number of neurons per area in the ipsilateral cortex after ScrCAST−PEG−CS or CAST−PEG−CS delivery (PDF)

## AUTHOR INFORMATION

### Corresponding Author

**Ester J. Kwon** − *Department of Bioengineering, University of California, La Jolla, California 92093, United States;* orcid.org/0000-0002-6335-9681; Email: ejkwon@ucsd.edu

### Authors

**Marianne I. Madias** − *Department of Bioengineering, University of California, La Jolla, California 92093, United States;* orcid.org/0000-0003-0127-7952

**Lilyane N. Stessman** − *Department of Bioengineering, University of California, La Jolla, California 92093, United States*

**Sophia J. Warlof** − *Department of Bioengineering, University of California, La Jolla, California 92093, United States*

**Julia A. Kudryashev** − *Department of Bioengineering, University of California, La Jolla, California 92093, United States;* orcid.org/0000-0003-3022-0058

Complete contact information is available at: https://pubs.acs.org/10.1021/acsnano.4c06052

### Notes

The authors declare no competing financial interest.

## ACKNOWLEDGMENTS

This work was supported by the National Science Foundation (NSF) CAREER Award (2046926) and the National Institutes of Health (NIH) Director's New Innovator Award (DP2NS111507). M.I.M. acknowledges support from the NSF Graduate Research Fellowship Program under grant no. DGE-2038238.

## REFERENCES

(1) Thurman, D. J. *Traumatic Brain Injury in the United States: A Report to Congress*; National Center for Injury Prevention and Control (U.S.) Division of Acute Care, Rehabilitation Research, and Disability Prevention, 1999. https://stacks.cdc.gov/view/cdc/13632.

(2) Peterson, A. B.; Xu, L.; Daugherty, J.; Breiding, M. J. *Surveillance Report of Traumatic Brain Injury-Related Emergency Department Visits, Hospitalizations, and Deaths, United States*; National Center for Injury Prevention and Control (U.S.), 2014. https://stacks.cdc.gov/view/cdc/78062.

(3) Menon, D. K.; Maas, A. I. R. Progress, Failures and New Approaches for TBI Research. *Nat. Rev. Neurol.* **2015**, *11* (2), 71−72.

(4) Skolnick, B. E.; Maas, A. I.; Narayan, R. K.; van der Hoop, R. G.; MacAllister, T.; Ward, J. D.; Nelson, N. R.; Stocchetti, N. A Clinical Trial of Progesterone for Severe Traumatic Brain Injury. *N. Engl. J. Med.* **2014**, *371* (26), 2467−2476.

(5) Wright, D. W.; Yeatts, S. D.; Silbergleit, R.; Palesch, Y. Y.; Hertzberg, V. S.; Frankel, M.; Goldstein, F. C.; Caveney, A. F.; Howlett-Smith, H.; Bengelink, E. M.; Manley, G. T.; Merck, L. H.; Janis, L. S.; Barsan, W. G. Very Early Administration of Progesterone for Acute Traumatic Brain Injury. *N. Engl. J. Med.* **2014**, *371* (26), 2457−2466.

(6) Stein, D. G. Embracing Failure: What the Phase III Progesterone Studies Can Teach about TBI Clinical Trials. *Brain Inj.* **2015**, *29* (11), 1259−1272.

(7) Korley, F.; Pauls, Q.; Yeatts, S. D.; Jones, C. M. C.; Corbett-Valade, E.; Silbergleit, R.; Frankel, M.; Barsan, W.; Cahill, N. D.; Bazarian, J. J.; Wright, D. W. Progesterone Treatment Does Not Decrease Serum Levels of Biomarkers of Glial and Neuronal Cell Injury in Moderate and Severe Traumatic Brain Injury Subjects: A Secondary Analysis of the Progesterone for Traumatic Brain Injury, Experimental Clinical Treatment (ProTECT) III Trial. *J. Neurotrauma* **2021**, *38* (14), 1953−1960.

(8) Poloyac, S. M.; Bertz, R. J.; McDermott, L. A.; Marathe, P. Pharmacological Optimization for Successful Traumatic Brain Injury Drug Development. *J. Neurotrauma* **2020**, *37* (22), 2435−2444.

(9) Kumar, A.; Loane, D. J. Neuroinflammation after Traumatic Brain Injury: Opportunities for Therapeutic Intervention. *Brain, Behav., Immun.* **2012**, *26* (8), 1191−1201.

(10) Ng, S. Y.; Lee, A. Y. W. Traumatic Brain Injuries: Pathophysiology and Potential Therapeutic Targets. *Front. Cell. Neurosci.* **2019**, *13*, 528.

(11) Alluri, H.; Grimsley, M.; Shaji, C. A.; Varghese, K. P.; Zhang, S. L.; Peddaboina, C.; Robinson, B.; Beeram, M. R.; Huang, J. H.; Tharakan, B. Attenuation of Blood-Brain Barrier Breakdown and Hyperpermeability by Calpain Inhibition. *J. Biol. Chem.* **2016**, *291* (53), 26958−26969.

(12) Kudryashev, J. A.; Waggoner, L. E.; Leng, H. T.; Mininni, N. H.; Kwon, E. J. An Activity-Based Nanosensor for Traumatic Brain Injury. *ACS Sens.* **2020**, *5* (3), 686−692.

(13) Saatman, K. E.; Creed, J.; Raghupathi, R. Calpain as a Therapeutic Target in Traumatic Brain Injury. *Neurotherapeutics* **2010**, *7* (1), 31−42.

(14) Cardali, S.; Maugeri, R. Detection of alphaII-Spectrin and Breakdown Products in Humans after Severe Traumatic Brain Injury. *J. Neurosurg. Sci.* **2006**, *50* (2), 25−31.

(15) Deng, Y.; Thompson, B. M.; Gao, X.; Hall, E. D. Temporal Relationship of Peroxynitrite-Induced Oxidative Damage, Calpain-Mediated Cytoskeletal Degradation and Neurodegeneration after Traumatic Brain Injury. *Exp. Neurol.* **2007**, *205* (1), 154−165.

(16) Jordán, J.; Galindo, M. F.; Miller, R. J. Role of Calpain- and Interleukin-1 Beta Converting Enzyme-like Proteases in the Beta-Amyloid-Induced Death of Rat Hippocampal Neurons in Culture. *J. Neurochem.* **1997**, *68* (4), 1335−1778.

(17) Villa, P. G.; Henzel, W. J.; Sensenbrenner, M.; Henderson, C. E.; Pettmann, B. Calpain Inhibitors, but Not Caspase Inhibitors, Prevent Actin Proteolysis and DNA Fragmentation during Apoptosis. *J. Cell Sci.* **1998**, *111* (6), 713−722.

(18) Pike, B. R.; Zhao, X.; Newcomb, J. K.; Wang, K. K. W.; Posmantur, R. M.; Hayes, R. L. Temporal Relationships between de Novo Protein Synthesis, Calpain and Caspase 3-like Protease Activation, and DNA Fragmentation during Apoptosis in Septo-Hippocampal Cultures. *J. Neurosci. Res.* **1998**, *52* (5), 505−520.

(19) Nath, R.; Raser, K. J.; McGinnis, K.; Nadimpalli, R.; Stafford, D.; W Wang, K. K. Effects of ICE-like Protease and Calpain Inhibitors on Neuronal Apoptosis. *Neuroreport* **1996**, *8* (1), 249−255.

(20) Thompson, S. N.; Carrico, K. M.; Mustafa, A. G.; Bains, M.; Hall, E. D. A Pharmacological Analysis of the Neuroprotective Efficacy of the Brain- and Cell-Permeable Calpain Inhibitor MDL-28170 in the Mouse Controlled Cortical Impact Traumatic Brain Injury Model. *J. Neurotrauma* **2010**, *27* (12), 2233−2243.

(21) Schoch, K. M.; Evans, H. N.; Brelsfoard, J. M.; Madathil, S. K.; Takano, J.; Saido, T. C.; Saatman, K. E. Calpastatin Overexpression Limits Calpain-Mediated Proteolysis and Behavioral Deficits Following Traumatic Brain Injury. *Exp. Neurol.* **2012**, *236* (2), 371−382.

(22) Wang, Y.; Liu, Y.; Lopez, D.; Lee, M.; Dayal, S.; Hurtado, A.; Bi, X.; Baudry, M. Protection against TBI-Induced Neuronal Death with Post-Treatment with a Selective Calpain-2 Inhibitor in Mice. *J. Neurotrauma* **2018**, *35* (1), 105−117.

(23) Schoch, K. M.; von Reyn, C. R.; Bian, J.; Telling, G. C.; Meaney, D. F.; Saatman, K. E. Brain Injury-Induced Proteolysis Is Reduced in a Novel Calpastatin Overexpressing Transgenic Mouse. *J. Neurochem.* **2013**, *125* (6), 909−920.

(24) Posmantur, R.; Kampfl, A.; Siman, R.; Liu, S.; Zhao, X.; Clifton, G. L.; Hayes, R. L. A Calpain Inhibitor Attenuates Cortical Cytoskeletal Protein Loss after Experimental Traumatic Brain Injury in the Rat. *Neuroscience* **1997**, *77* (3), 875−888.

(25) Yu, C. G.; Bondada, V.; Joshi, A.; Reneer, D. V.; Telling, G. C.; Saatman, K. E.; Geddes, J. W. Calpastatin Overexpression Protects against Excitotoxic Hippocampal Injury and Traumatic Spinal Cord Injury. *J. Neurotrauma* **2020**, *37* (21), 2268−2276.

(26) Tao, X.-G.; Shi, J.-H.; Hao, S.-Y.; Chen, X.-T.; Liu, B.-Y. Protective Effects of Calpain Inhibition on Neurovascular Unit Injury through Downregulating Nuclear Factor-κB-Related Inflammation during Traumatic Brain Injury in Mice. *China Med. J.* **2017**, *130* (2), 187−198.

(27) Ma, M.; Shofer, F. S.; Neumar, R. W. Calpastatin Over-expression Protects Axonal Transport in an In Vivo Model of Traumatic Axonal Injury. *J. Neurotrauma* **2012**, *29* (16), 2555−2563.

(28) Markgraf, C. G.; Velayo, N. L.; Johnson, M. P.; McCarty, D. R.; Medhi, S.; Koehl, J. R.; Chmielewski, P. A.; Linnik, M. D. Six-Hour Window of Opportunity for Calpain Inhibition in Focal Cerebral Ischemia in Rats. *Stroke* **1998**, *29* (1), 152−158.

(29) Wang, Y.; Liu, Y.; Bi, X.; Baudry, M. Calpain-1 and Calpain-2 in the Brain: New Evidence for a Critical Role of Calpain-2 in Neuronal Death. *Cells* **2020**, *9* (12), 2698.

(30) Wang, Y.; Liu, Y.; Nham, A.; Sherbaf, A.; Quach, D.; Yahya, E.; Ranburger, D.; Bi, X.; Baudry, M. Calpain-2 as a Therapeutic Target

in Repeated Concussion-Induced Neuropathy and Behavioral Impairment. *Sci. Adv.* **2020**, *6* (27), No. eaba5547.
(31) Baudry, M.; Wang, Y.; Bi, X.; Luo, Y. L.; Wang, Z.; Kamal, Z.; Shirokov, A.; Sullivan, E.; Lagasca, D.; Khalil, H.; Lee, G.; Fosnaugh, K.; Bey, P.; Mehdi, S.; Coulter, G. Identification and Neuroprotective Properties of NA-184, a Calpain-2 Inhibitor. *Pharmacol. Res. Perspect.* **2024**, *12* (2), No. e1181.
(32) Cagmat, E. B.; Guingab-Cagmat, J. D.; Vakulenko, A. V.; Hayes, R. L.; Anagli, J. Potential Use of Calpain Inhibitors as Brain Injury Therapy. In *Brain Neurotrauma: Molecular, Neuropsychological, and Rehabilitation Aspects*; Kobeissy, F. H., Ed.; Frontiers in Neuroengineering; CRC Press/Taylor & Francis: Boca Raton (FL), 2015.
(33) Pietsch, M.; Chua, K. C. H.; Abell, A. D. Calpains: Attractive Targets for the Development of Synthetic Inhibitors. *Curr. Top. Med. Chem.* **2010**, *10* (3), 270−293.
(34) Ma, M. Role of Calpains in the Injury-Induced Dysfunction and Degeneration of the Mammalian Axon. *Neurobiol. Dis.* **2013**, *60*, 61−79.
(35) Betts, R.; Weinsheimer, S.; Blouse, G. E.; Anagli, J. Structural Determinants of the Calpain Inhibitory Activity of Calpastatin Peptide B27-WT. *J. Biol. Chem.* **2003**, *278* (10), 7800−7809.
(36) Hall, E. D.; Sullivan, P. G.; Gibson, T. R.; Pavel, K. M.; Thompson, B. M.; Scheff, S. W. Spatial and Temporal Characteristics of Neurodegeneration after Controlled Cortical Impact in Mice: More than a Focal Brain Injury. *J. Neurotrauma* **2005**, *22* (2), 252−265.
(37) Newcomb, J. K.; Kampfl, A.; Posmantur, R. M.; Zhao, X.; Pike, B. R.; Liu, S. J.; Clifton, G. L.; Hayes, R. L. Immunohistochemical Study of Calpain-Mediated Breakdown Products to α-Spectrin Following Controlled Cortical Impact Injury in the Rat. *J. Neurotrauma* **1997**, *14* (6), 369−383.
(38) Launey, Y.; Fryer, T. D.; Hong, Y. T.; Steiner, L. A.; Nortje, J.; Veenith, T. V.; Hutchinson, P. J.; Ercole, A.; Gupta, A. K.; Aigbirhio, F. I.; Pickard, J. D.; Coles, J. P.; Menon, D. K. Spatial and Temporal Pattern of Ischemia and Abnormal Vascular Function Following Traumatic Brain Injury. *JAMA Neurol.* **2020**, *77* (3), 339.
(39) Beitchman, J. A.; Lifshitz, J.; Harris, N. G.; Thomas, T. C.; Lafrenaye, A. D.; Hånell, A.; Dixon, C. E.; Povlishock, J. T.; Rowe, R. K. Spatial Distribution of Neuropathology and Neuroinflammation Elucidate the Biomechanics of Fluid Percussion Injury. *Neurotrauma Rep.* **2021**, *2* (1), 59−75.
(40) Ringger, N. C.; Tolentino, P. J.; McKinsey, D. M.; Pike, B. R.; Wang, K. K. W.; Hayes, R. L. Effects of Injury Severity on Regional and Temporal mRNA Expression Levels of Calpains and Caspases after Traumatic Brain Injury in Rats. *J. Neurotrauma* **2004**, *21* (7), 829−841.
(41) Saatman, K. E.; Bozyczko-Coyne, D.; Marcy, V.; Siman, R.; McIntosh, T. K. Prolonged Calpain-Mediated Spectrin Breakdown Occurs Regionally Following Experimental Brain Injury in the Rat. *J. Neuropathol. Exp. Neurol.* **1996**, *55* (7), 850−860.
(42) McGinn, M. J.; Kelley, B. J.; Akinyi, L.; Oli, M. W.; Liu, M. C.; Hayes, R. L.; Wang, K. K. W.; Povlishock, J. T. Biochemical, Structural, and Biomarker Evidence for Calpain-Mediated Cytoskeletal Change After Diffuse Brain Injury Uncomplicated by Contusion. *J. Neuropathol. Exp. Neurol.* **2009**, *68* (3), 241−249.
(43) Rink, A.; Fung, K. M.; Trojanowski, J. Q.; Lee, V. M.; Neugebauer, E.; McIntosh, T. K. Evidence of Apoptotic Cell Death after Experimental Traumatic Brain Injury in the Rat. *Am. J. Pathol.* **1995**, *147* (6), 1575−1583.
(44) Conti, A. C.; Raghupathi, R.; Trojanowski, J. Q.; McIntosh, T. K. Experimental Brain Injury Induces Regionally Distinct Apoptosis during the Acute and Delayed Post-Traumatic Period. *J. Neurosci.* **1998**, *18* (15), 5663−5672.
(45) Vasiljeva, O.; Menendez, E.; Nguyen, M.; Craik, C. S.; Michael Kavanaugh, W. Monitoring Protease Activity in Biological Tissues Using Antibody Prodrugs as Sensing Probes. *Sci. Rep.* **2020**, *10* (1), 5894.
(46) Vandooren, J.; Geurts, N.; Martens, E.; Van den Steen, P. E.; Opdenakker, G. Zymography Methods for Visualizing Hydrolytic Enzymes. *Nat. Methods* **2013**, *10* (3), 211−220.
(47) Zhao, X.; Newcomb, J. K.; Pike, B. R.; Hayes, R. L. Casein Zymogram Assessment of μ-Calpain and m-Calpain Activity After Traumatic Brain Injury in the Rat In Vivo. In *Calpain Methods and Protocols*; Humana Press: NJ, 2000; Vol. *144*, pp 117−120.
(48) Agrawal, S.; Anderson, P.; Durbeej, M.; van Rooijen, N.; Ivars, F.; Opdenakker, G.; Sorokin, L. M. Dystroglycan Is Selectively Cleaved at the Parenchymal Basement Membrane at Sites of Leukocyte Extravasation in Experimental Autoimmune Encephalomyelitis. *J. Exp. Med.* **2006**, *203* (4), 1007−1019.
(49) Gerwien, H.; Hermann, S.; Zhang, X.; Korpos, E.; Song, J.; Kopka, K.; Faust, A.; Wenning, C.; Gross, C. C.; Honold, L.; Melzer, N.; Opdenakker, G.; Wiendl, H.; Schäfers, M.; Sorokin, L. Imaging Matrix Metalloproteinase Activity in Multiple Sclerosis as a Specific Marker of Leukocyte Penetration of the Blood-Brain Barrier. *Sci. Transl. Med.* **2016**, *8* (364), 364ra152.
(50) Fonović, M.; Bogyo, M. Activity-Based Probes as a Tool for Functional Proteomic Analysis of Proteases. *Expert Rev. Proteomics* **2008**, *5* (5), 721−730.
(51) Kwong, G. A.; Dudani, J. S.; Carrodeguas, E.; Mazumdar, E. V.; Zekavat, S. M.; Bhatia, S. N. Mathematical Framework for Activity-Based Cancer Biomarkers. *Proc. Natl. Acad. Sci. U.S.A.* **2015**, *112* (41), 12627−12632.
(52) Kwong, G. A.; von Maltzahn, G.; Murugappan, G.; Abudayyeh, O.; Mo, S.; Papayannopoulos, I. A.; Sverdlov, D. Y.; Liu, S. B.; Warren, A. D.; Popov, Y.; Schuppan, D.; Bhatia, S. N. Mass-Encoded Synthetic Biomarkers for Multiplexed Urinary Monitoring of Disease. *Nat. Biotechnol.* **2013**, *31* (1), 63−70.
(53) Kwon, E. J.; Dudani, J. S.; Bhatia, S. N. Ultrasensitive Tumour-Penetrating Nanosensors of Protease Activity. *Nat. Biomed. Eng.* **2017**, *1* (4), 0054−110.
(54) Kandell, R. M.; Kudryashev, J. A.; Kwon, E. J. Targeting the Extracellular Matrix in Traumatic Brain Injury Increases Signal Generation from an Activity-Based Nanosensor. *ACS Nano* **2021**, *15* (12), 20504−20516.
(55) Kudryashev, J. A.; Madias, M. I.; Kandell, R. M.; Lin, Q. X.; Kwon, E. J. An Activity-Based Nanosensor for Minimally-Invasive Measurement of Protease Activity in Traumatic Brain Injury. *Adv. Funct. Mater.* **2023**, *33* (28), 2300218.
(56) Hanna, R. A.; Campbell, R. L.; Davies, P. L. Calcium-Bound Structure of Calpain and Its Mechanism of Inhibition by Calpastatin. *Nature* **2008**, *456* (7220), 409−412.
(57) Wendt, A.; Thompson, V. F.; Goll, D. E. Interaction of Calpastatin with Calpain: A Review. *Biol. Chem.* **2004**, *385* (6), 465−472.
(58) Wang, T.; Wang, L.; Moreno-Vinasco, L.; Lang, G. D.; Siegler, J. H.; Mathew, B.; Usatyuk, P. V.; Samet, J. M.; Geyh, A. S.; Breysse, P. N.; Natarajan, V.; Garcia, J. G. N. Particulate Matter Air Pollution Disrupts Endothelial Cell Barrier via Calpain-Mediated Tight Junction Protein Degradation. *Part. Fibre Toxicol.* **2012**, *9* (1), 35.
(59) Kawasaki, H.; Emori, Y.; Imajoh-Ohmi, S.; Minami, Y.; Suzuki, K. Identification and Characterization of Inhibitory Sequences in Four Repeating Domains of the Endogenous Inhibitor for Calcium-Dependent Protease. *J. Biochem.* **1989**, *106* (2), 274−281.
(60) Maki, M.; Bagci, H.; Hamaguchi, K.; Ueda, M.; Murachi, T.; Hatanaka, M. Inhibition of Calpain by a Synthetic Oligopeptide Corresponding to an Exon of the Human Calpastatin Gene. *J. Biol. Chem.* **1989**, *264* (32), 18866−18869.
(61) Stockholm, D.; Bartoli, M.; Sillon, G.; Bourg, N.; Davoust, J.; Richard, I. Imaging Calpain Protease Activity by Multiphoton FRET in Living Mice. *J. Mol. Biol.* **2005**, *346* (1), 215−222.
(62) Baudry, M.; Bi, X. Calpain-1 and Calpain-2: The Yin and Yang of Synaptic Plasticity and Neurodegeneration. *Trends Neurosci.* **2016**, *39* (4), 235−245.
(63) Perrin, C.; Vergely, C.; Zeller, M.; Rochette, L. In Vitro Antioxidant Properties of Calpain Inhibitors: Leupeptin and Calpain Inhibitor-1. *Cell Mol. Biol.* **2002**, *48*, OL267−270.


https://doi.org/10.1021/acsnano.4c06052
*ACS Nano* 2024, 18, 25565−25576

(64) Bihovsky, R.; Tao, M.; Mallamo, J. P.; Wells, G. J. 1,2-Benzothiazine 1,1-Dioxide α-Ketoamide Analogues as Potent Calpain I Inhibitors. *Bioorg. Med. Chem. Lett.* **2004**, *14*, 1035−1038.
(65) Levesque, S.; Wilson, B.; Gregoria, V.; Thorpe, L. B.; Dallas, S.; Polikov, V. S.; Hong, J.-S.; Block, M. L. Reactive Microgliosis: Extracellular μ-Calpain and Microglia-Mediated Dopaminergic Neurotoxicity. *Brain* **2010**, *133* (3), 808−821.
(66) Osier, N. D.; Dixon, C. E. The Controlled Cortical Impact Model: Applications, Considerations for Researchers, and Future Directions. *Front. Neurol.* **2016**, *7*, 134.
(67) Kadota, E.; Muramatsu, Y.; Nonaka, K.; Karasuno, M.; Nishi, K.; Dote, K.; Hashimoto, S. Biological Functions of Extravasated Serum IgG in Rat Brain. *Acta Neurochir. Suppl.* **2000**, *76*, 69−72.
(68) Cash, A.; Theus, M. H. Mechanisms of Blood-Brain Barrier Dysfunction in Traumatic Brain Injury. *Int. J. Mol. Sci.* **2020**, *21* (9), 3344.
(69) Saatman, K. E.; Graham, D. I.; McIntosh, T. K. The Neuronal Cytoskeleton Is at Risk After Mild and Moderate Brain Injury. *J. Neurotrauma* **1998**, *15* (12), 1047−1058.
(70) Newcomb, J. K.; Zhao, X.; Pike, B. R.; Hayes, R. L. Temporal Profile of Apoptotic-like Changes in Neurons and Astrocytes Following Controlled Cortical Impact Injury in the Rat. *Exp. Neurol.* **1999**, *158* (1), 76−88.
(71) Momeni, H. R. Role of Calpain in Apoptosis. *Cell J.* **2011**, *13* (2), 65−72.
(72) Saatman, K. E.; Feeko, K. J.; Pape, R. L.; Raghupathi, R. Differential Behavioral and Histopathological Responses to Graded Cortical Impact Injury in Mice. *J. Neurotrauma* **2006**, *23* (8), 1241−1253.
(73) Podbielska, M.; Das, A.; Smith, A. W.; Chauhan, A.; Ray, S. K.; Inoue, J.; Azuma, M.; Nozaki, K.; Hogan, E. L.; Banik, N. L. Neuron-Microglia Interaction Induced Bi-Directional Cytotoxicity Associated with Calpain Activation. *J. Neurochem.* **2016**, *139* (3), 440−455.
(74) Pike, B. R.; Zhao, X.; Newcomb, J. K.; Posmantur, R. M.; Wang, K. K.; Hayes, R. L. Regional Calpain and Caspase-3 Proteolysis of α-Spectrin after Traumatic Brain Injury. *NeuroReport* **1998**, *9* (11), 2437−2442.
(75) Anderson, K. J.; Miller, K. M.; Fugaccia, I.; Scheff, S. W. Regional Distribution of Fluoro-Jade B Staining in the Hippocampus Following Traumatic Brain Injury. *Exp. Neurol.* **2005**, *193* (1), 125−130.
(76) Gao, X.; Deng-Bryant, Y.; Cho, W.; Carrico, K. M.; Hall, E. D.; Chen, J. Selective Death of Newborn Neurons in Hippocampal Dentate Gyrus Following Moderate Experimental Traumatic Brain Injury. *J. Neurosci. Res.* **2008**, *86* (10), 2258−2270.
(77) Clark, R. S. B.; Kochanek, P. M.; Chen, M.; Watkins, S. C.; Marion, D. W.; Chen, J.; Hamilton, R. L.; Loeffert, J. E.; Graham, S. H. Increases in Bcl-2 and Cleavage of Caspase-1 and Caspase-3 in Human Brain after Head Injury. *FASEB J.* **1999**, *13* (8), 813−821.
(78) Gao, X.; Enikolopov, G.; Chen, J. Moderate Traumatic Brain Injury Promotes Proliferation of Quiescent Neural Progenitors in the Adult Hippocampus. *Exp. Neurol.* **2009**, *219* (2), 516−523.
(79) Ngwenya, L. B.; Danzer, S. C. Impact of Traumatic Brain Injury on Neurogenesis. *Front. Neurosci.* **2019**, *12*, 1014.
(80) Wang, X.; Gao, X.; Michalski, S.; Zhao, S.; Chen, J. Traumatic Brain Injury Severity Affects Neurogenesis in Adult Mouse Hippocampus. *J. Neurotrauma* **2016**, *33* (8), 721−733.


https://doi.org/10.1021/acsnano.4c06052
*ACS Nano* 2024, 18, 25565−25576